Available online at www.sciencedirect.com
SCIENCE DIRECT®
PERGAMON
Automatica 39 (2003) 1037–1044
automatica
www.elsevier.com/locate/automatica

Brief Paper

A set theoretic approach for time-to-contact estimation in dynamic vision☆

M. Di Marco, A. Garulli, D. Prattichizzo, A. Vicino*

Dipartimento di Ingegneria dell'Informazione, Università di Siena, Via Roma 56, 53100 Siena, Italy

Received 4 February 2002; received in revised form 3 October 2002; accepted 4 February 2003

Abstract

This paper deals with the estimation of the time-to-contact in dynamic vision. It is well known that differential invariants of the image velocity field can be used to characterize the shape changes of objects in the scene, due to relative motion between the observer and the scene. Under the hypothesis of constant velocity along the optical axis, the time-to-contact turns out to be a function of the area enclosed by the object contour and its time derivative.

In the paper, a novel approach based on set membership estimation theory is proposed to estimate the variables involved in the computation of the time-to-contact. Both errors in the motion model and image measurement noise are described as unknown-but-bounded disturbances, without requiring any statistical assumption. The proposed technique allows for the computation of guaranteed bounds on the time-to-contact estimates in finite time, a crucial issue in all problems where a robust evaluation of the time-to-contact is in order.

Keywords: Dynamic vision; Set membership; Estimation; Time-to-contact; Contour tracking

1. Introduction

One of the main problems in robot visual navigation and in robot manipulation systems is the computation of the time-to-contact. In mobile robotics, the recovery of this parameter is of paramount importance in collision avoidance and in braking. The work of Nelson and Aloimonos (1988) is one of the first papers where vision-based spatio-temporal techniques enable the robotic device to avoid collisions by computing the time-to-contact (see Cipolla (1996) for a comprehensive bibliography on the topic).

The basic problem consists in computing the time needed for the observer to reach a fixed object, in the hypothesis that the relative velocity along the optical axis is kept constant. Within the world of dynamic vision, this specific problem appears as a typical "goal-oriented" problem, in the sense that its solution does not require the complete 3-D scene reconstruction, but it can be accomplished in an efficient way by using only a partial solution of the general structure-from-motion problem. Differential invariants of the image velocity field (curl, divergence and shear) are used to characterize the changes in the shape of objects in the scene due to the relative motion between the observer and the scene. Under the hypothesis of constant velocity along the optical axis, the time-to-contact turns out to be a function of the area enclosed by the object contour and its time derivative. One advantage of this method is that the evaluation of the time-to-contact is performed without tracking point features in the image, i.e. without estimating the full image velocity field, which is an ill-conditioned problem. In fact, since the estimates are based on surface integrals along the contours, the area-based method is weakly sensitive to noise measurements. The main drawback of this technique consists in its sensitivity to partial occlusions of the object.

The aim of the present paper is twofold. First, a new recursive estimation technique is introduced for evaluating the variables involved in the computation of the time-to-contact. The new technique relies on a recently developed approach to estimation problems, known as *set membership* or *unknown-but-bounded* approach (see e.g.

☆ This paper was not presented at any IFAC meeting. This paper was recommended for publication by Associate Editor Keum-shik Hong under the direction of Editor Mituhiko Araki.

* Corresponding author.
E-mail address: vicino@ing.unisi.it (A. Vicino).

0005-1098/03/$ - see front matter © 2003 Elsevier Science Ltd. All rights reserved.
doi:10.1016/S0005-1098(03)00062-1

Schweppe, 1973; Milanese & Vicino, 1991; Garulli, Tesi, & Vicino, 1999). The basic assumption underlying this theory is that error and noise processes belong to prescribed sets. The objective is to find optimal set estimators and evaluate the corresponding minimal uncertainty intervals for the unknown variables to be estimated.

The second contribution of the paper consists in providing theoretical results which allow for the computation of guaranteed uncertainty intervals for the time-to-contact estimate in a finite number of steps. This topic is important in all the problems where an explicit evaluation of the accuracy of the estimate of the time-to-contact is crucial (a typical example being obstacle avoidance in autonomous navigation).

The paper is organized as follows. Section 2 introduces the set membership technique used to track contours parameterized according to B-splines snakes. Section 3 solves the problem of evaluating nonconservative uncertainty intervals for the time-to-contact estimates. Experimental results are presented and discussed in Section 4, while Section 5 reports some concluding remarks.

2. Contour tracking and differential invariants approach

2.1. Parameterization of image contours

Linear parameterization of image contours is largely used in computer vision. B-splines interpolation shows attractive features for fitting both open and closed contours (see e.g. Blake, Curwen, & Zisserman, 1993; Blake & Isard, 1998). In fact, it is well known that this parameterization leads to numerically well-behaved solutions and to efficient algorithms.

A closed B-spline curve of degree h is defined as

$$\mathscr{S}(u)=\sum_{i=0}^{m-1} V_i B_{ih}(u), \qquad u\in[u_{\min},u_{\max}],$$

where $B_{ih}(u)$ are the B-spline base functions of degree h and the coefficients $V_i=(X_i,Y_i)$ are the *control points* of the curve.

The contour tracking problem consists in computing an estimate $\hat{\mathscr{S}}(u;t)$ of the object contour as a function of the control points $V_i(t)$, evolving dynamically with time. The problem is frequently approached through Kalman filtering. This is done by constructing a state space model of the rigid object contour motion. State variables are defined as the coordinates $X_i(t)$, $Y_i(t)$ of the control points and their respective time derivatives $\dot{X}_i(t)$, $\dot{Y}_i(t)$.

The visual measurement process consists in collecting measurements of the contour position, by searching along directions orthogonal to the estimated curve and within a search window, whose size is function of the positional variance of the current estimate. Contour measurements can be expressed in terms of control points as

$$z_x(u,t)=[B(u)\quad 0]\begin{bmatrix}X\\ \dot{X}\end{bmatrix}+v_x(u,t), \tag{1}$$

where v_x is the measurement noise, $B(u)$ is a vector whose components are the B-spline base functions $B_{ih}(u)$, $i=0,\dots,m-1$ and $X=[X_0,\dots,X_{m-1}]'$. A similar equation holds for measurements $z_y(u,t)$ of the second coordinate of the control points.

If the image shape is complex, the parameterization through B-splines requires a large number of control points. As a consequence, the dimension of the state space vector dramatically increases, leading image tracking algorithms to instability (Blake et al., 1993). For many purposes, like, for example, the computation of the time-to-contact, the objects to be tracked are usually planar rigid bodies, as for instance the area of the rear windscreen of a car in automatic parking applications. In such cases, the contour parameterization can be simplified. In fact the projection onto the image plane of a planar rigid object, moving with respect to the camera, can be approximated by just six affine degrees of freedom, under the hypothesis of *weak perspective*, i.e. if the depth of the object is small with respect to its distance from the camera, or when the planar object is orthogonal to the optical axis (a quite common situation in time-to-contact evaluation). The six degrees of freedom can be represented by a vector Q defined as $Q=[t_x\ \ t_y\ \ sr_{11}\ \ sr_{22}\ \ sr_{21}\ \ sr_{12}]'$, where t_x (t_y) represents the coefficient of the contour translation in the image plane along the x (y) direction, s denotes the scaling factor and r_{ij} is the (i,j) entry of the rotation matrix R ($\det(R)=1$).

The Q-parameterization describes the contour as a function of the *template* (Fischler & Elschlager, 1973), i.e. the initial reference estimated contour denoted by control points $(\bar{X},\bar{Y})$. The relationship between the Q vector and the control points of a single captured image is given by

$$\begin{bmatrix}X\\ Y\end{bmatrix}=WQ, \qquad W=\begin{bmatrix}c_x\underline{1} & 0 & \bar{X} & 0 & 0 & \bar{Y}\\ 0 & c_y\underline{1} & 0 & \bar{Y} & \bar{X} & 0\end{bmatrix}, \tag{2}$$

where $\underline{1}=[11\dots1]'$, and (c_x,c_y) is a reference point in the image (usually, the rotation center for the planar rigid motion of the image). Clearly, the initial contour is represented by the vector $Q_0=[0\ \ 0\ \ 1\ \ 1\ \ 0\ \ 0]'$.

The 12-dimensional vector of state variables to be estimated is defined as $[Q'\ \ \dot{Q}']'$, $\dot{Q}$ being the time derivative of Q. The contour dynamics in the affine state space is easily obtained from the corresponding dynamic equations in the control points state space. As regards the visual measurements process, Eq. (1) and its y counterpart turn into

$$\begin{bmatrix}z_x(u,t)\\ z_y(u,t)\end{bmatrix}=\left[\begin{pmatrix}B(u) & 0\\ 0 & B(u)\end{pmatrix}W\ \middle|\ 0\right]\begin{bmatrix}Q\\ \dot{Q}\end{bmatrix}+\begin{bmatrix}v_x(u,t)\\ v_y(u,t)\end{bmatrix}.$$

2.2. Discrete-time dynamics of image contour

In order to derive a tracking algorithm for the image contour, the discrete-time version of the contour dynamics and the measurement equation should be considered. The discrete-time equations take on the following general form:

$$\lambda_{k+1} = F_k\lambda_k + G_k w_k,$$

$$y_k = H\lambda_k + v_k, \tag{3}$$

where $\lambda_k = [Q' \;\; \dot{Q}']'$ represents the state vector at time k and w_k (v_k) is the process (measurement) noise. The $2L$ visual measurements available at time k are grouped into the vector $y_k = [z_x(u_1,k) \;\; z_y(u_1,k) \;\; \cdots \;\; z_x(u_L,k) \;\; z_y(u_L,k)]'$ and the output matrix H can be written as $H = [\bar{H} \;\; 0]$ where

$$\bar{H} = \left[W' \begin{pmatrix} B(u_1) & 0 \\ 0 & B(u_1) \end{pmatrix} \ldots W' \begin{pmatrix} B(u_L) & 0 \\ 0 & B(u_L) \end{pmatrix} \right]'.$$

The measurement noise vector is $v_k = [v_x(u_1,k), \;\; v_y(u_1,k) \ldots v_x(u_L,k), v_y(u_L,k)]'$.

Matrices F_k and G_k reflect the a priori knowledge on the contour dynamics. In particular, F_k represents the deterministic part of the dynamics and accounts for information about different motion components in the image plane, such as translation, rotation and scaling. On the other hand, G_k explains how random acceleration terms affect the contour dynamics. For example, let us consider the case of uniform motion towards the geometric center of the contour of a fixed planar rigid object. The projected image will undergo a simple expansion, with no translation and rotation. In the affine transformation parameterization introduced in Section 2.1, this contour motion is described by the state vector $Q(t) = [1 - s(t) \;\; 1 - s(t) \;\; s(t) \;\; s(t) \;\; 0 \;\; 0]'$, where the scale factor $s(t) = d_0/(d_0 - vt)$ is evaluated as the ratio between the distance from the object at time $t = 0$ (d_0) and that at time t, v being the (constant) velocity of the uniform motion. The presence of unknown acceleration terms can be accounted by the continuous-time model

$$\ddot{s}(t) = 2\frac{v}{d_0}\dot{s}(t)s(t) + w(t). \tag{4}$$

Therefore, matrices F_k and G_k can be obtained by linearizing model (4) in $s(t)$ and then discretizing the linearized model (where $t = k\Delta$ and Δ is the chosen sampling time). Notice that as d_0 and/or v are usually unknown, the obtained linear time-varying model is not a priori known. A possible choice is to replace $s(k\Delta)$ with an estimate $\hat{s}(k\Delta)$, previously computed on the basis of the collected visual measurements up to time $(k-1)\Delta$.

2.3. Contour tracking via set membership filtering

Following an alternative approach with respect to the literature, in this paper we assume that both process and measurement noises in (3) are unknown-but-bounded (Milanese & Vicino, 1991). This means that the a priori knowledge on uncertainty affecting the system can be expressed as

$$\|w_k\|_\infty \leqslant \varepsilon_w, \qquad \|v_k\|_\infty \leqslant \varepsilon_v, \tag{5}$$

where ε_w and ε_v are known positive scalars and $\|a\|_\infty \triangleq \sup_i |a_i|$. Weighted ∞-norms and time-varying bounds can be also considered in (5), thus including complex dynamics errors and spatially varying measurement noise in the proposed framework. Notice that no statistical assumptions are made on w_k and v_k. This permits to treat also biased and/or nonstationary disturbances, for which a rich a priori knowledge is required. Actually, in many practical cases, it is considerably easier to get knowledge on error magnitude bounds.

In this setting, the problem of computing a recursive estimate of the state vector can be addressed in a set theoretic approach, see e.g. Bertsekas and Rhodes (1971), Chernousko (1980), Chisci, Garulli, and Zappa (1996). Assume that the initial state vector λ_0 lies in the bounded set $\mathscr{X}(0|-1)$, i.e., the a priori knowledge on the initial conditions. Then, denote by $\mathscr{X}(k|k)$ and $\mathscr{X}(k+1|k)$ the sets of state vectors λ_k and λ_{k+1}, respectively, which are compatible with all the available information up to time k (namely the noise bounds (5), the initial condition $\mathscr{X}(0|-1)$ and the measurements y_i, for $i = 0, 1, \ldots, k$). It is easy to see that the above sets are generated by the following recursion:

$$\mathscr{X}(k|k) = \mathscr{X}(k|k-1) \cap \mathscr{M}(k),$$

$$\mathscr{X}(k+1|k) = F_k\mathscr{X}(k|k) + G_k\mathscr{S}_\infty(\varepsilon_w),$$

where $\mathscr{M}(k) = \{\lambda_k : \|y_k - H\lambda_k\|_\infty \leqslant \varepsilon_v\}$ is the set of state vectors compatible with the measurements at time k, and $\mathscr{S}_\infty(\varepsilon_w)$ is the ball of radius ε_w in the ∞-norm.

In general, as k increases, the sets $\mathscr{X}(k|k)$ and $\mathscr{X}(k+1|k)$ become very complicated and their exact computation requires a large amount of calculations. Therefore, approximation through simple regions like ellipsoids is often pursued. In this paper, the approximating regions adopted are *parallelotopes*. An n-dimensional parallelotope is defined as $\mathscr{P} = \{\lambda \in \mathbb{R}^n : \lambda = \hat{\lambda} + T\alpha, \; \|\alpha\|_\infty \leqslant 1\}$ where $\hat{\lambda}$ is the center of the parallelotope and T is the $n \times n$ matrix whose column vectors represent the edges of the parallelotope.

Recursive approximation of polytopic regions through parallelotopes has been introduced in Vicino and Zappa (1996), and then applied to the state estimation problem in Chisci et al. (1996), where two sequences of outer approximating parallelotopes $\mathscr{P}(k|k)$ and $\mathscr{P}(k+1|k)$ are computed so that they satisfy the inclusions

$$\mathscr{P}(0|-1) \supseteq \mathscr{X}(0|-1),$$

$$\mathscr{P}(k|k) \supseteq \mathscr{P}(k|k-1) \cap \mathscr{M}(k),$$

$$\mathscr{P}(k+1|k) \supseteq F_k\mathscr{P}(k|k) + G_k\mathscr{S}_\infty(\varepsilon_w).$$

In order to reduce the conservativeness introduced by the approximation, minimum-volume parallelotopes are considered. Hence, at time k, the set theoretic parallelotopic state

filter provides the set estimate

$$\mathscr{P}(k|k) = \{\lambda_{k|k}: \lambda_{k|k} = \hat{\lambda}_{k|k} + T_{k|k}\alpha,\ \|\alpha\|_\infty \leqslant 1\}, \tag{6}$$

where $\hat{\lambda}_{k|k}$ is the central estimate of the state vector and $T_{k|k}$ defines the parallelotopic uncertainty region associated to the central estimate. The uncertainty intervals relative to each state variable can be obtained by computing the minimum-volume axis-aligned box containing the parallelotope $\mathscr{P}(k|k)$. The desired outbounding box is provided by the following lemma, which can be easily proven.

Lemma 1. *Consider the parallelotope $\mathscr{P}(k|k)$ in (6), and let $T_{k|k} = \{t_{ij}\}$. Then, the minimum-volume axis-aligned box containing $\mathscr{P}(k|k)$ is given by*

$$\mathscr{B}(k|k) = \{\lambda_{k|k}: \lambda_{k|k} = \hat{\lambda}_{k|k} + D_{k|k}\alpha,\ \|\alpha\|_\infty \leqslant 1\},$$

where $D_{k|k} = \mathrm{diag}\{d_1, d_2, \ldots\}$ and $d_i = \sum_j |t_{ij}|$.

2.4. Computation of the time-to-contact

The time-to-contact τ is defined as the time interval between the present instant and the instant when the observing sensor and the point on the object along the optical axis come to collision, under the hypothesis of uniform relative motion.

Denoting by $A(t)$ the area enclosed by the contour estimated at time t, and by $\dot{A}(t)$ its time derivative, it can be shown that the time-to-contact τ is given by (Cipolla, 1996)

$$\tau = \frac{2A(t)}{\dot{A}(t)}. \tag{7}$$

From Green's theorem in the plane it is easy to show that the area enclosed by a curve with parameterization $X(u)$ and $Y(u)$ is given by $A(t) = \int_{u_{\min}}^{u_{\max}} X(u;t)(\mathrm{d}/\mathrm{d}u)Y(u;t)\,\mathrm{d}u$. In the case of contour parameterization through B-splines control points, it can be shown that

$$A(t) = \sum_i \sum_j (X_i Y_j) \int_{u_{\min}}^{u_{\max}} B_{ik} \frac{\mathrm{d}}{\mathrm{d}u} B_{jk}\,\mathrm{d}u.$$

In matrix notation one gets $A(t) = X'(t)SY(t)$ and its time derivative: $\dot{A}(t) = \dot{X}'(t)SY(t) + X'(t)S\dot{Y}(t)$, where $S = \{s_{ij}\}$, $s_{ij} = \int_{u_{\min}}^{u_{\max}} B_{ik}(\mathrm{d}/\mathrm{d}u)B_{jk}\,\mathrm{d}u$.

Consider the Q-parameterization introduced in Section 2.1 and partition equation (2) as $X = W_x Q$, $Y = W_y Q$. Then, the area contained in the image contour and its derivative become

$$A(t) = Q' W_x' S W_y Q, \tag{8}$$

$$\dot{A}(t) = Q'(W_x' S W_y + W_y' S' W_x)\dot{Q}. \tag{9}$$

Note that $A(t)$ and $\dot{A}(t)$ can be estimated quite inexpensively at any iteration of the set membership filter recursion described in Section 2.3. In fact, $Q, \dot{Q}$ are exactly the state variables of the contour dynamics model. Moreover, since the entries of matrix S are integral parameters which do not depend on time t, they can be computed off-line not affecting the computational burden of the tracking algorithm.

Due to the particular structure of matrices W_x and W_y, the diagonal elements of matrix $W_x' S W_y$ are zero. Therefore, $A(t)$ and $\dot{A}(t)$ turn out to be multilinear functions of the state vector $[Q'\ \dot{Q}']$ components. Multilinearity will play a key role in computing the bounds on the time-to-contact estimate (see Section 3).

3. Set-theoretic time-to-contact estimate

Let $\mathscr{B}$ be the estimated uncertainty box for the parameters Q and their time derivatives. Following Lemma 1, this set can be written as $\mathscr{B} = \{\lambda \in \mathbb{R}^{12}: \hat{\lambda}_i - d_i \leqslant \lambda_i \leqslant \hat{\lambda}_i + d_i\}$.

From (7)–(9), it ensues that, the time-to-contact is given by the ratio of two multilinear functions in the state space variables, i.e.

$$\tau(\lambda) = \frac{2A(t)}{\dot{A}(t)} = \frac{n[\lambda(t)]}{d[\lambda(t)]}. \tag{10}$$

Now, we want to compute the uncertainty interval $[\tau_{\min}, \tau_{\max}]$ on the time-to-contact, induced by uncertainty in the parameter vector λ, i.e. we want to solve the following constrained optimization problems

$$\tau_{\min} = \min_{\lambda \in \mathscr{B}} \tau(\lambda), \qquad \tau_{\max} = \max_{\lambda \in \mathscr{B}} \tau(\lambda). \tag{11}$$

Notice that problems (11) are nonconvex, being the objective function the ratio of two multilinear functions of the independent variables. We show in the following that both problems (11) can be solved in a finite number of steps. Let us introduce a special extremal subset of $\mathscr{B}$, containing the vertices of the hyperrectangle $\mathscr{B}$

$$\mathscr{B}_v = \{\lambda \in \mathscr{B}: \lambda_i = \hat{\lambda}_i + \alpha_i d_i,\ \alpha_i \in \{-1, 1\}\}.$$

Lemma 2. *Let $f(\lambda): R^{\mathrm{M}} \to R$ be a multilinear function of λ. Then*

$$\max_{\lambda \in \mathscr{B}} f(\lambda) = \max_{\lambda \in \mathscr{B}_v} f(\lambda), \qquad \min_{\lambda \in \mathscr{B}} f(\lambda) = \min_{\lambda \in \mathscr{B}_v} f(\lambda).$$

Now, we can state and prove the main result of this section.

Theorem 1. *Let the time-to-contact τ be defined as in (10), via (8) and (9). Moreover, let $\mathrm{d}(\lambda) \neq 0$, $\forall \lambda \in \mathscr{B}$. Then*

$$\tau_{\min} = \min_{\lambda \in \mathscr{B}_v} \tau(\lambda), \qquad \tau_{\max} = \max_{\lambda \in \mathscr{B}_v} \tau(\lambda).$$

Proof. With reference to the definition of τ in (10), let us introduce the function $F(\tau; \lambda) = \tau\,\mathrm{d}(\lambda) - n(\lambda)$.

For a fixed τ, define the value set $\mathscr{V}(\tau) = \{x \in \mathbb{R}: x = F(\tau; \lambda),\ \text{for some } \lambda \in \mathscr{B}\}$. The set $\mathscr{V}(\tau)$ is a segment of the real axis, whose left and right endpoints are

$$E^{\mathrm{l}}(\tau) = \min_{\lambda \in \mathscr{B}} F(\tau; \lambda), \qquad E^{\mathrm{r}}(\tau) = \max_{\lambda \in \mathscr{B}} F(\tau; \lambda).$$

From the definition of τ in (10), it is easy to verify that $0 \in \mathscr{V}(\tau)$, if and only if $\tau_{\min} \leqslant \tau \leqslant \tau_{\max}$. By a continuity argument, the minimum and maximum values of τ for which the equation $F(\tau;\lambda) = 0$ admits a solution for some $\tilde{\lambda} \in \mathscr{B}$, are values of τ such that one of the endpoints of the value set $\mathscr{V}(\tau)$ coincides with the origin of the real axis. This means $E^{\mathrm{r}}(\tau_{\min}) = 0$ or $E^{\mathrm{l}}(\tau_{\min}) = 0$, and similarly $E^{\mathrm{r}}(\tau_{\max}) = 0$ or $E^{\mathrm{l}}(\tau_{\max}) = 0$. Since the function $F(\tau;\lambda)$ is multilinear in λ, by Lemma 2 it is concluded that for any fixed τ, and hence also for $\tau = \tau_{\min}$ and $\tau = \tau_{\max}$, there exist $\lambda_v^m, \lambda_v^{\mathrm{M}} \in \mathscr{B}_v$ such that

$$\lambda_v^m = \arg\{\min_{\lambda \in \mathscr{B}} F(\tau;\lambda)\}, \qquad \lambda_v^{\mathrm{M}} = \arg\{\max_{\lambda \in \mathscr{B}} F(\tau;\lambda)\}.$$

This completes the proof. □

Clearly, if there exists $\bar{\lambda} \in \mathscr{B}$ such that $\mathrm{d}(\bar{\lambda}) = 0$, one has $\tau_{\max} = +\infty$, while $\tau_{\min}$ is still given by (11).

Once the bounds $\tau_{\min}$ and $\tau_{\max}$ have been computed, a natural estimate of τ in (7) is given by the center of the uncertainty interval, i.e.

$$\hat{\tau} = \frac{\tau_{\min} + \tau_{\max}}{2}.$$

4. Experimental results

This section reports results of experiments performed in order to test the algorithm presented in the previous section on both artificial and real sequences of images.

4.1. Simulation results

A first experiment has been performed by using a set of simulated images obtained moving a virtual camera at constant speed, along the optical axis and towards the geometric center of the contour of a synthetic object (see Fig. 1a)

As motion model, a linear time-varying discrete linearization of Eq. (4) has been adopted with an initial estimate $\hat{\tau}_0$ of the time-to-contact, generally different from the true value $\tau_0 = \tau(0) = d_0/v$. Obviously, the closer the initial estimate to the true time-to-contact, the better the model prediction. Beside $\hat{\tau}_0$, the other tuning parameters of the set membership algorithm are the bounds on w_k and v_k. These bounds

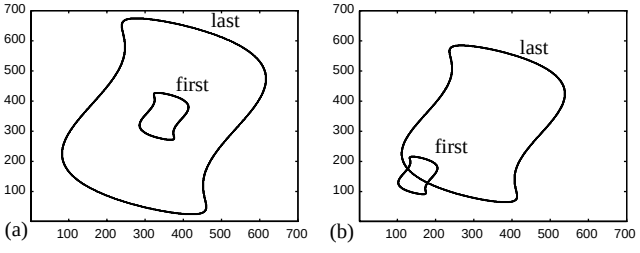

Fig. 1. Contours of the first and last images of two testing sequences: (a) camera motion towards the geometric center of the image contour; (b) camera motion towards a point on the image contour.

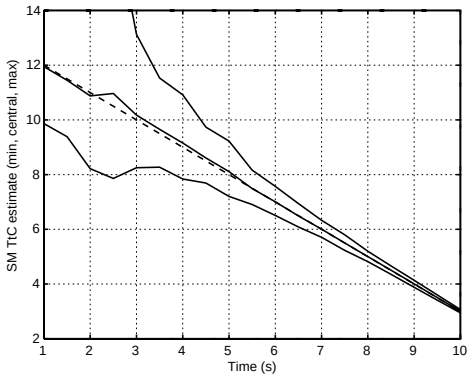

Fig. 2. Set membership time-to-contact estimate in the case of exact a priori knowledge $\hat{\tau}_0 = \tau(0)$. True time-to-contact (dashed); nominal estimate (solid central); error bounds (solid outer).

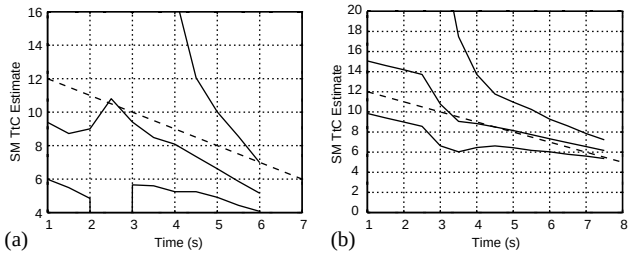

Fig. 3. (a) Time-to-contact in the case of a priori knowledge $\hat{\tau}_0 > \tau(0)$: true time-to-contact (dashed); nominal estimate (solid central); error bounds (solid outer). (b) Estimate in the case $\hat{\tau}_0 < \tau(0)$: true time-to-contact (dashed), nominal estimate (solid central); error bounds (solid outer).

represent the confidence level in the model structure and the measurement accuracy, respectively.

Fig. 2 shows the results of the set membership filter for the case when it is assumed that $\hat{\tau}_0 = \tau(0)$ (exact initial condition). In this case, the model is well tuned, and consequently, ε_w can be chosen small with respect to ε_v. The algorithm provides both good nominal central estimates for τ and tight bounds on that value (up to less than $\frac{1}{5}$ of the sampling time, here set to 0.5 s).

Fig. 3 shows the results for the case when the value of the parameter $\hat{\tau}_0$ is different from the true value of the time-to-contact at $t = 0$. Fig. 3a (3b) reports simulation results for $\hat{\tau}_0 = 9.5$ ($\hat{\tau}_0 = 15.5$), while the true value is 12.5. In these cases, the model will under-estimate (over-estimate) the true time-to-contact; due to the strong divergent behavior of the solution of Eq. (4), the model prediction dominates the measurement update, no matter how large (i.e., unreliable) is the value of the model error $\boldsymbol{\varepsilon}_w$. As a consequence, there exists a time instant when the feasible set provided by the algorithm becomes empty, and this will cause a break in the recursive procedure. It is interesting to note that the set membership filter can be tuned in order to stop when the true value is outside the bounds provided by the algorithm (see Fig. 3). This feature can be used to verify the reliability

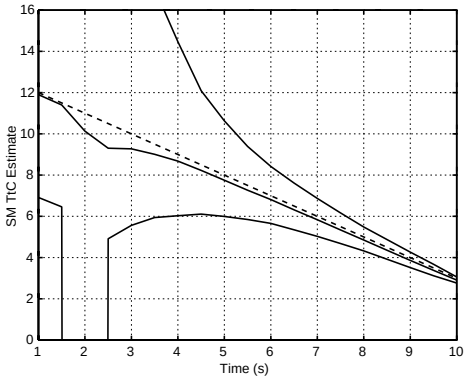

Fig. 4. Motion not aligned with the center of the image. True time-to-contact (dashed); nominal estimates and lower and upper bounds (solid).

of the model itself, and surely is one of its most appealing features (see Section 4.2).

The algorithm has been tested also on a sequence of synthetic images for which the optical axis does not cross the geometric center of the object shape (see Fig. 1b). In this case, model (4) is not able to describe the translational motion added to the optical axis-aligned motion. As a consequence, there exists a drift introducing an error on both measurement and model updates. In Fig. 4, results are shown for $\hat{\tau}_0 = \tau(0)$ and for an experiment with motion along an axis not intersecting the center of the image. Apart from the first four steps, needed to estimate the drifting component, the estimates exhibit the same behavior as in the first experiment (Fig. 2).

4.2. Comparison with Kalman filter approach

The performance of the set membership algorithm has been compared to that of the classical Kalman filter. As it is well known, the two approaches are quite different. Set membership provides hard bounds on the state estimates using parallelotopes; Kalman filtering provides confidence ellipsoids for the estimates, under the assumption that all noises are Gaussian.

In order to fairly compare the two methods, the covariance matrices of the Kalman filter has been chosen so that it is possible to establish a relationship between the noise-bounding boxes defined by (5) for the set membership filter, and the 99.9% confidence ellipsoid for Gaussian noises in the Kalman filter approach. In particular, two different choices have been considered for the noise confidence ellipsoids: (i) the maximum-volume ellipsoids completely contained in the noise boxes; (ii) ellipsoids with the same shape and volume as the corresponding noise boxes. First, the ideal case reported at the beginning of Section 4.1, under the hypothesis $\hat{\tau}_0 = \tau(0)$ has been examined. In this case, the Kalman filter provides better performances than the set membership algorithm: the former shows faster convergence and gives

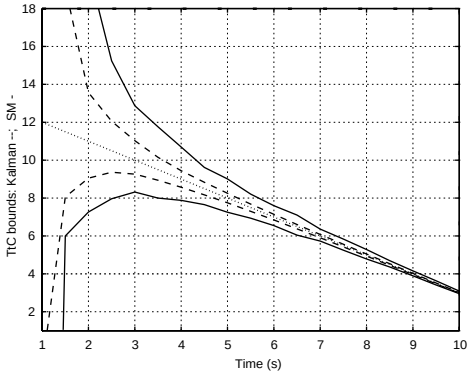

Fig. 5. Bounds provided by set membership (solid) and Kalman filtering (dashed) in the ideal case ($\hat{\tau}_0 = \tau(0)$); true time-to-contact (dotted).

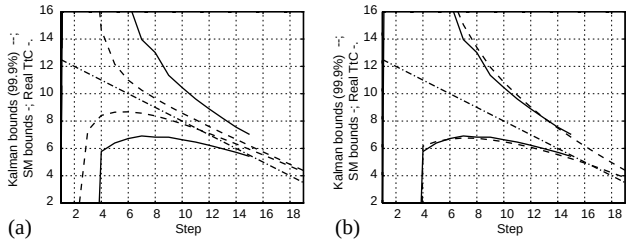

Fig. 6. Bounds provided by set membership (solid) and Kalman (dashed) algorithms (true time-to-contact is dash-dotted) in the case $\hat{\tau}_0 > \tau(0)$. (a) Inner confidence ellipsoids; (b) Equivolume confidence ellipsoids.

tighter bounds (Fig. 5). Note that for both approaches lower and upper bounds on the time-to-contact are evaluated on the minimum volume box containing the parallelotope (set membership) and the confidence ellipsoid (Kalman) according to Theorem 1.

The specific features of the set membership algorithm become more evident when the experimental setting is closer to a realistic setup. This is shown in Fig. 6,where it is assumed that the initial estimate $\hat{\tau}_0$ is larger than the true value $\tau(0)$. Consider the case where inner bounding noise confidence ellipsoids are used. It is easily verified that while the set membership filter always gives guaranteed bounds and stops when the true time-to-contact is no longer inside the bounds, the Kalman filtering approach provides tighter but incorrect bounds. Fig. 6a reports a case in which from time step 11 on, the true time-to-contact is outside the Kalman bounds.

The same situation arises when one considers larger noise confidence ellipsoids. Fig. 6b reports the results for the case when boxes and ellipsoids with equal volume are considered. In this case, the bounds provided by the two algorithms are almost identical. Nevertheless, while the set membership algorithm is capable of detecting when the true time-to-contact exceeds the estimated error bounds, the Kalman filter cannot do the same (see time instant 17 in Fig. 6b).

4.3. Real experiments

The algorithm has been tested on real image sequences, obtained through a camera mounted on a robotic arm and

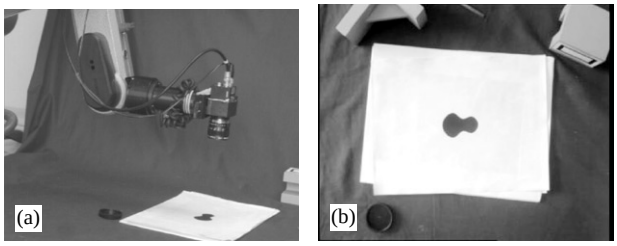

Fig. 7. (a) Experimental setup. (b) First image of the sequence.

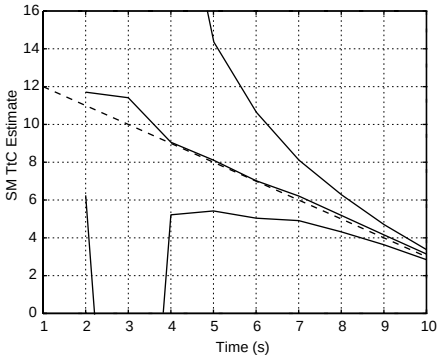

Fig. 8. Algorithm results for the experimental setup in Fig. 7. (a) True time-to-contact (dashed); central estimates (solid central); error bounds (solid outer).

approaching a highly contrasted shape (see Fig. 7). In this case, the sampling time is relatively large (1 s), and only few images are available. Hence, the filter is required to provide accurate estimates and reliable bounds in few steps. The results provided by the set membership filter are shown in Fig. 8: notice how, after a transient of just four steps, the algorithm converges to a good estimate, while tightening the bounds down to less then one half of the sampling time.

Not surprisingly, the experimental results show that whenever the observation time is limited and the sampling time cannot be made sufficiently small, a good estimate for the initial condition $\tau(0)$ is crucial for reliability of the recursive estimates. To improve the behavior of the algorithm during the transient and its tracking performances, one could employ an adaptive linear discretization of the uniform motion model (4). The basic idea is to exploit the current time-to-contact estimate to update the system model. This can be done without introducing significant changes in the computational complexity of the algorithm. Using the aforementioned strategy, the algorithm can better tolerate an inaccurate initial estimate and recover more efficiently from possible accidental deviations of the estimates from their expected behavior. The adaptive algorithm has been tested on the setting of Fig. 7. Fig. 9 shows the algorithm outputs for $\hat{\tau}_0$ varying from 60% to 150% of the true value $\tau(0)$. It can be observed that the adaptive algorithm is now able to tune its internal model providing a good estimate of the time-to-contact, despite the poor a priori knowledge on the initial condition.

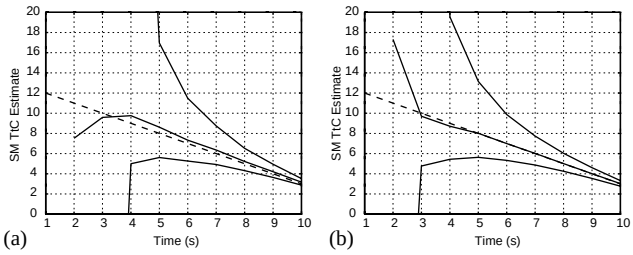

Fig. 9. Testing the adaptive algorithm on real data: (a) $\hat{\tau}_0 = 0.58\,\tau(0)$; (b) $\hat{\tau}_0 = 1.5\tau(0)$.

5. Conclusions

The estimation of the time-to-contact has been approached in a set membership framework. A new algorithm has been devised for tracking object contours and estimating the variables involved in the evaluation of the time-to-contact. The proposed set membership filter provides guaranteed error bounds on the estimates and this is of paramount importance in robotic applications like obstacle avoidance in autonomous navigation.

Comparisons with the classical Kalman filter approach show that the set membership estimation algorithm is particularly useful in those cases where significant errors in the motion model are present, while it is not excessively conservative in standard conditions when the Kalman filter is the optimal estimator. Experimental results on both synthetic and real sequences are encouraging and suggest that the proposed method can be a reliable and powerful alternative to existent time-to-contact estimation techniques.

References

Bertsekas, D. P., & Rhodes, I. B. (1971). Recursive state estimation for a set-membership description of uncertainty. *IEEE Transactions on Automatic Control*, *16*, 117–128.

Blake, A., Curwen, R., & Zisserman, A. (1993). A framework for spatio-temporal control in the tracking of visual contours. *International Journal of Computer Vision*, *11*, 127–145.

Blake, A., & Isard, M. (1998). *Active contours*. Berlin: Springer.

Chernousko, F. L. (1980). Optimal guaranteed estimates of indeterminacies with the aid of ellipsoids. Part I. *Engineering Cybernetics*, *18*, 1–9.

Chisci, L., Garulli, A., & Zappa, G. (1996). Recursive state bounding by parallelotopes. *Automatica*, *32*, 1049–1055.

Cipolla, R. (1996). Active visual inference of surface shape. In *Lecture notes in computer science*, Vol. 1016. Berlin: Springer.

Fischler, M. A., & Elschlager, R. A. (1973). The representation and matching of pictorial structures. *IEEE Transactions on Computers*, 22, 67–92.

Garulli, A., Tesi, A., & Vicino, A. (Eds.) (1999). *Robustness in identification and control.* Lecture notes in control and information sciences. London: Springer.

Milanese, M., & Vicino, A. (1991). Optimal estimation theory for dynamic systems with set membership uncertainty: An overview. *Automatica*, *27*(6), 997–1009.

Nelson, R. C., & Aloimonos, J. (1988). Using flow field divergence for obstacle avoidance: Towards qualitative vision. In *Proceedings of the Second International Conference on Computer Vision*, Tarpon Springs, FL; USA (pp. 188–196).

Schweppe, F. C. (1973). *Uncertain dynamic systems*. Englewood Cliffs, NJ: Prentice-Hall.

Vicino, A., & Zappa, G. (1996). Sequential approximation of feasible parameter sets for identification with set membership uncertainty. *IEEE Transactions on Automatic Control*, *41*, 774–785.

Mauro Di Marco was born in Firenze, Italy, in 1970. He received the Laurea Degree in electronic engineering from the University of Firenze, Firenze, Italy and the Ph.D. degree from the University of Bologna, Bologna, Italy, in 1997 and 2001, respectively.

Since 2000 he has been with the University of Siena, Siena, Italy, where he is currently Assistant Professor of Circuit Theory.

From November 1999 to April 2000 he held a visiting position at LAAS, Toulouse, France. His current research interests are in analysis of nonlinear dynamics of complex systems and neural networks, in robust estimation and filtering, and in autonomous navigation.

Andrea Garulli was born in Bologna, Italy, in 1968. He received the Laurea in Electronic Engineering from the Universita' di Firenze in 1993, and the Ph.D. in System Engineering from the Universita' di Bologna in 1997. In 1996 he joined the Dipartimento di Ingegneria dell'Informazione of the Universita' di Siena, where he is currently Associate Professor.

He has been member of the Conference Editorial Board of the IEEE Control Systems Society from 2000 to 2002. He presently serves as Associate Editor for the IEEE Transactions on Automatic Control.

He is author of more than 60 technical publications and co-editor of the book "Robustness in Identification and Control", Springer, 1999. His present research interests include robust identification and estimation, robust control, LMI-based optimization, mobile robotics and autonomous navigation.

Domenico Prattichizzo received the M.S. degree in Electronics Engineering and the Ph.D. degree in Robotics and Automation from the University of Pisa, Pisa, Italy in 1991 and 1995, respectively.

Since 2002 he is Associate Professor of Robotics and Automation at the University of Siena. In 1994, he was Visiting Scientist at the Artificial Intelligence Laboratory at Massachusetts Institute of Technology, Cambridge. Since 1992, he is a Research Associate in the Robotics and Automation group at the Centro "E.Piaggio" of the University of Pisa. He was co-organizer and chairman of many sessions on robotics and control theory in many International Conferences. He was co-chair of the Second IEEE International Workshop on Control Problems in Robotics and Automation (Las Vegas, December 2002). He has been invited to give talks in many International Conferences. Since 2001, he serves as Member of the Editorial Board of the Journal of Dynamics of Continuous, Discrete and Impulsive Systems (DCDIS) Series B: Application and Algorithms and as Member of the Conference Editorial Board of the IEEE Control System Society. Prof. Prattichizzo is co-editor of the book "Control Problems in Robotics", vol. 4, STAR, Springer Tracks in Advanced Robotics, Springer Verlag, 2003. He is co-author of more than 90 papers in the area of robotics and automation.

Antonio Vicino was born in 1954. He received the Laurea in Electrical Engineering from the Politecnico di Torino, Torino, Italy, in 1978. From 1979 to 1982 he held several Fellowships at the Dipartimento di Automatica e Informatica of the Politecnico di Torino. He was assistant professor of Automatic Control from 1983 to 1987 at the same Department. From 1987 to 1990 he was Associate Professor of Control Systems at the Universita' di Firenze. In 1990 he joined the Dipartimento di Ingegneria Electrica, Universita' di L'Aquila, as Professor of Control Systems. Since 1993 he is with the Universita' di Siena, where he founded the Dipartimento di Ingegneria dell'Informazione and covered the position of Head of the Department from 1996 to 1999. From 1999 he has been Dean of the Engineering Faculty. In 2000 he founded the Center for Complex Systems Studies (CSC) of the University of Siena, where he presently covers the position of Director.

He has served as Associate Editor for the IEEE Transactions on Automatic Control from 1992 to 1996. Presently he serves as Associate Editor for Automatica and Associate Editor at Large for the IEEE Transactions on Automatic Control. He is Fellow of the IEEE.

He is author of 170 technical publications, co-editor of 2 books on 'Robustness in Identification and Control', Guest Editor of the Special Issue 'Robustness in Identification and Control' of the Int. Journal of Robust and Nonlinear Control. He has worked on stability analysis of nonlinear systems and time series analysis and prediction. Presently, his main research interests include robust control of uncertain systems, robust identification and filtering, mobile robotics and applied system modelling.